plasma technology for metals oxide synthesis and composited with salt as degrade catalyst of polystyrene

Safaa M. Atallah, Ibraheem J. Ibraheem
Chemistry Department, College of Science, University of Anbar
saf20s3002@uoanbar.edu.iq

Abstract:

Every year, millions of tons of plastic waste grow up in the environment, contributing to global warming, the deaths of numerous species, and an increase in both animal and human illnesses.Pollution formed by polystyrene is one type of waste.This work uses a plasma technique to generate nickel oxide and barium oxide nanoparticles. The data were examined usingatomic absorption spectrometry (AAS), field emission scanning electron microscopy (FE-SEM), and UV- visible spectroscopy (UV). In the tests mentioned above, the average size of the created barium oxide nanoparticles was 45.73 nm while the average size of the created nickel oxide nanoparticles was 40.37 nm.Then, using the produced nanoparticles, we made saline nanocomposites. Different nanocomposites were created utilizing various nickel oxide nanoparticle concentrations (25.3, 50.6, and 75.9 ppm). In addition to the creation of several nanocomposites utilizing varying concentrations of barium oxide nanoparticles (25.9, 51.9, and 77.8 ppm), 20 ml of methanol and 3 g of nickel chloride were added with stirring for 48 hours for each concentration mentioned.our study including improving the thermal degradation products of polymers by using the above-prepared salt nanocomposites with different concentrations. In each experiment, one of the above concentrations is added to polystyrene. From thermal decomposition by simple distillation, we obtained a liquid fuel from each experiment at 280 °C and 350 °C. We note that the decomposition time decreases with an increasing concentration of nanocomposites.For polystyrene decomposition products at 280 °C by using the above-prepared salt nanocomposites with different concentrations. We obtained a liquid that has some of the high properties of the fuel. As the concentration of the nanocomposite increases, we note: an increase in the volume of the product; a decrease in density and viscosity; an increase in aniline point, and an increase in the octane number, especially with 104.7 at 25.3 ppm for NiO and 104.8 at 25.9 ppm for BaO; The cetane number is zero for all concentrations. For polystyrene decomposition products at 350 °C using NiO or BaO nanocomposites at different concentrations, we note: decreases in the product volume, density, and viscosity; an increase in the octane number, especially with 105 for both 50.6 ppm for NiO and 77.8 ppm for BaO; the cetane number is zero for all concentrations.

DOI Number: 10.14704/nq.2022.20.11.NQ66204 **NeuroQuantology 2022; 20(11): 2089-2098**

1- Introduction

With the increasing growth of the world's population, the demand and need for polymeric materials have increased, corresponding to an increase in the accumulation of non-biodegradable waste that causes harmful effects on the environment and human health, whether it is household waste or industrial waste [(1)]. Plastic waste is one of the most common types of polymeric waste, especially the main types of plastic that are used to manufacture materials for daily human consumption, such as high-density polyethylene, low-density polyethylene, polypropylene, polystyrene, polyvinyl chloride, and polyethylene terephthalate [(2)]. Plastic consumption has quadrupled during the past 30 years due to the increase in demand for plastic products and the doubled annual global production of plastic, rising from 234 million tons in 2000 to 396 million tons in 2016 and reaching 460 million tons in 2019. The annual growth of plastic consumption shows that the estimated global consumption of plastic by 2050 will exceed 500 million tons [(3)].

2- Polystyrene

Polystyrene (PS) is formed from the polymerization of styrene and has the molecular structure shown in Figure (1) which consists of repeating units of the formula $(C_8H_8)_n$. due to its good properties in terms of hardness, transparency, high refractive index, good electrical insulation properties, ease of processing, etc [(4)]. Polystyrene is widely used in packaging, toys, plastic cutlery, electrical and electronic insulators, CD boxes, and in the manufacture of refrigerators and cooling devices, and many others. As a result of its chemical stability and its spread everywhere, causing pollution to the environment due to its accumulation, new recycling or disposal processes must be sought in order to reduce the accumulation of PS [(5)].

eISSN 1303-5150

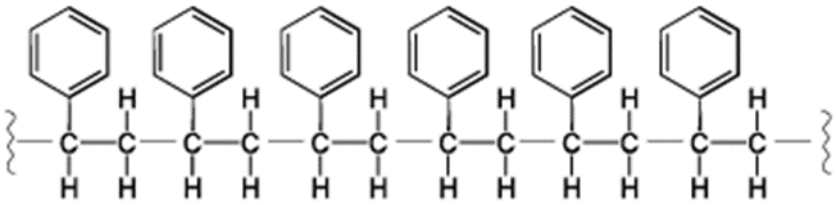

Figure (1): Molecular structure of polystyrene [4].

3- Materials and methods

3-1- Preparation of Barium and nickel Oxides nanoparticles by a plasma

It is possible to create nanoparticles by cold plasma between two electrodes in an atmosphere [6]. The plasma system consisted of a high voltage (5500 volts) and the flow of argon gas was graded from (0.5 to 5 cm^3/sec) and was controlled by a flow meter in the plasma system seen in Figure (2). The plasma torch is created between two electrodes; the top electrode serves as a capillary needle to enter argon gas and join it with electricity, and the lower electrode is submerged 1 cm after the plasma torch is made. Ionization of the fluid and the formation of nanoparticles take place under the plasma discharge.

Figure (2): Cold plasma system component.

Barium (II) chloride dihydrate (HIMedia India) is a chemical that may be used to make barium oxide nanoparticles when the concentration is 2800 ppm. The 0.50 g of ($BaCl_2.2H_2O$) was dissolved in 50 ml of deionized water (Chem-LabIraq) and exposed to a plasma torch for 45 minutes, causing the colorless solution to transform brown. Then we separated the precipitate by centrifuge 12,000 cycles/min (Tomos H-1650\USA) and repeated the process multiple times until we obtained the required amount of the precipitate.

The chemical nickel(II) chloride hexahydrate (HIMediaIndia) was used to make nickel oxide nanoparticles in the same manner as described previously, but at a concentration of 2000 ppm. The 0.40 g of ($NiCl_2.6H_2O$) was dissolved in 50 ml of deionized water (Chem-LabIraq), and after 45 minutes of exposure to a plasma torch, the solution's dark green colour turned to yellow. Then we separated the precipitate by centrifuge 12,000 cycles/min (Tomos H-1650\USA) and repeated the process multiple times until we obtained the required amount of the precipitate.

3-2- Preparation of BaO\NaCl and NiO\NaCl nanocomposite

By using atomic absorption spectroscopy (Phoenix 986\USA), the concentrations of the produced nickel oxide nanoparticles (1013 ppm) and barium oxide nanoparticles (2595 ppm) were measured. We take varied concentrations of 25.9, 51.9, and 77.8 ppm barium oxide nanoparticle solution, mix them with 3 g of NaCl (PanReac AppliChem, USA) and 20 ml of methanol (Banreac, Spain), and stir them for 48 hours to create the BaO\NaCl nanocomposites. For each concentration above, the procedure is repeated after which the result is separated and dried.

NiO\NaCl nanocomposites are created by combining varying concentrations of 25.3, 50.6, and 75.9 ppm of the nickel oxide

eISSN 1303-5150

nanoparticles solution, mix them with 3 g of NaCl (PanReac AppliChem, USA) and 20 ml of methanol (Banreac, Spain), and stir them for 48 hours. For each concentration above, the procedure is repeated after which the result is separated and dried.

3-3- Decomposition of polymeric waste into fuel

There are many ways to decompose polymeric waste, such as natural methods that take decades, like UV-visible rays from the sun, wind, rain, microorganisms, etc., as well as industrial methods such as cracking, decomposition, and recycling. In this paper, a simple distillation method was used to decompose polymeric waste [(7)].

Simple distillation is the process of turning a liquid material into steam by heating it to high temperatures and then condensing the vapor into a pure liquid by touching a cool surface (condenser) [(8)], as seen in figure (3). Waste polystyrene white cork was used. In each experiment, 100 g of polystyrene is placed in the distillation flask, and two products are obtained from each experiment at 280 °C and 350 °C. The first experiment was a distillation of polystyrene alone, and the following experiments added different concentrations of NiO\NaCl nanocomposites (25.3, 50.6, and 75.9 ppm) in order, as well as adding different concentrations of

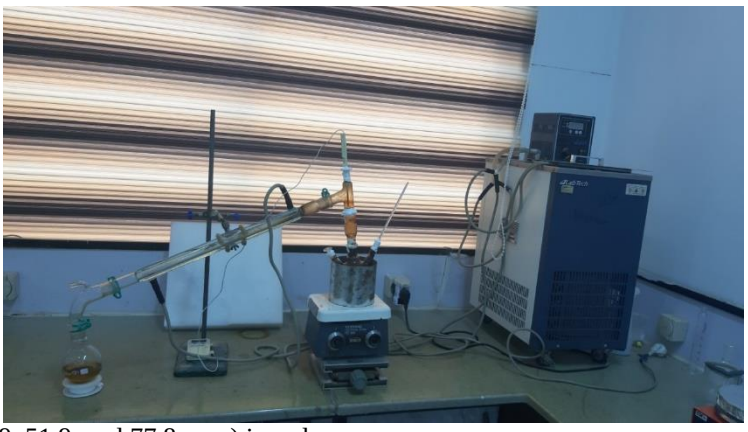

BaO\NaCl nanocomposites (25.9, 51.9, and 77.8 ppm) in order.

Figure (3): distillation system.

4- Results and discussion

4-1- Characterization of nanoparticles

4-1-1 Field emission scanning electron microscope (FE-SEM)

4-1-1-1 FE-SEM for Barium oxide nanoparticles

The form of barium oxide nanoparticles at 100 nm is seen in Figure (4). We got semi-spherical grains in barium oxide with average grain sizes between (45.73 and 117.07) nanometers.

eISSN 1303-5150

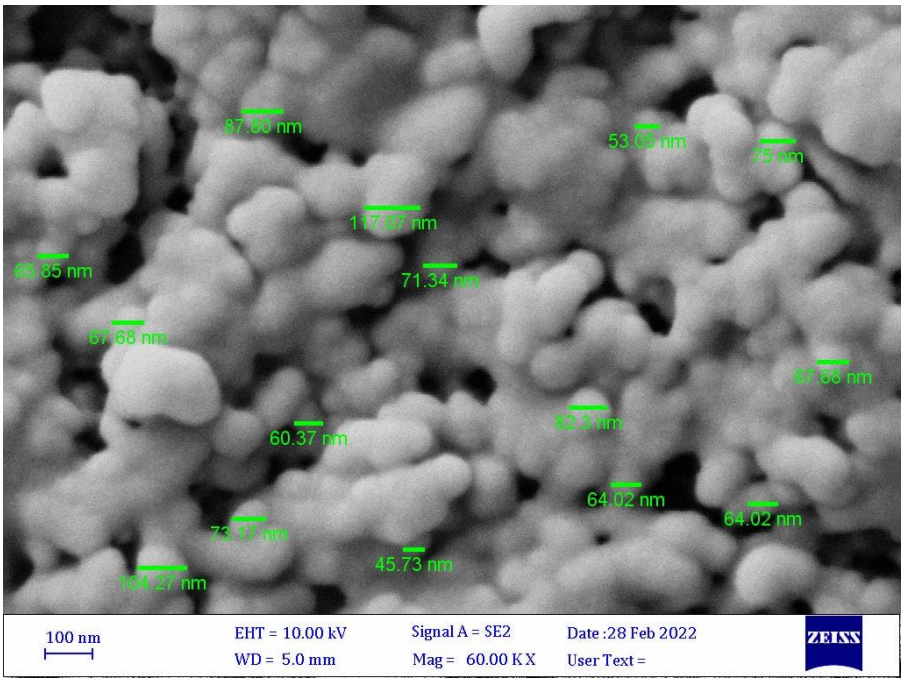

Figure (4): FE-SEM for Barium oxide nanoparticles (100 nm).

4-1-1-2 FE-SEM for nickel oxide nanoparticles

The form of nickel oxide nanoparticles at 100 nm is seen in Figure (5). We got semi-spherical nickel oxide grains with average grain

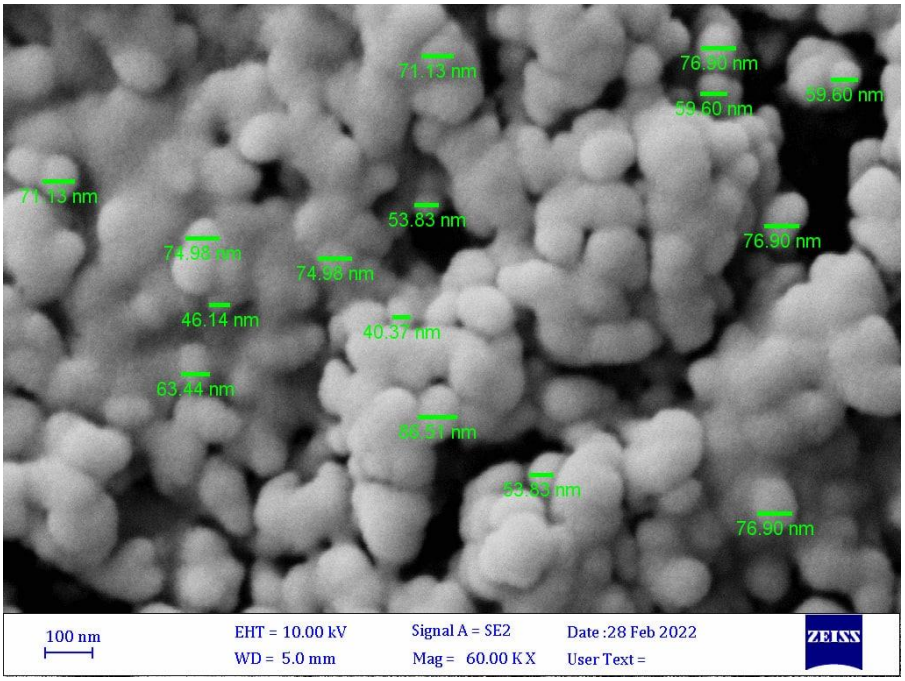

sizes between (40.37 and 86.51) nanometers.

Figure (5): FE-SEM for nickel oxide nanoparticles (100 nm).

4-1-2 UV-visible spectroscopy measurement

4-1-2-1 UV-visible of Barium Oxide nanoparticles

The UV-visible spectra of the produced barium nanoparticles are shown in Figure (6), with the maximum absorption peaking at 310 nm, which is consistent with the findings of researcher M. Ansari et al [(9)].

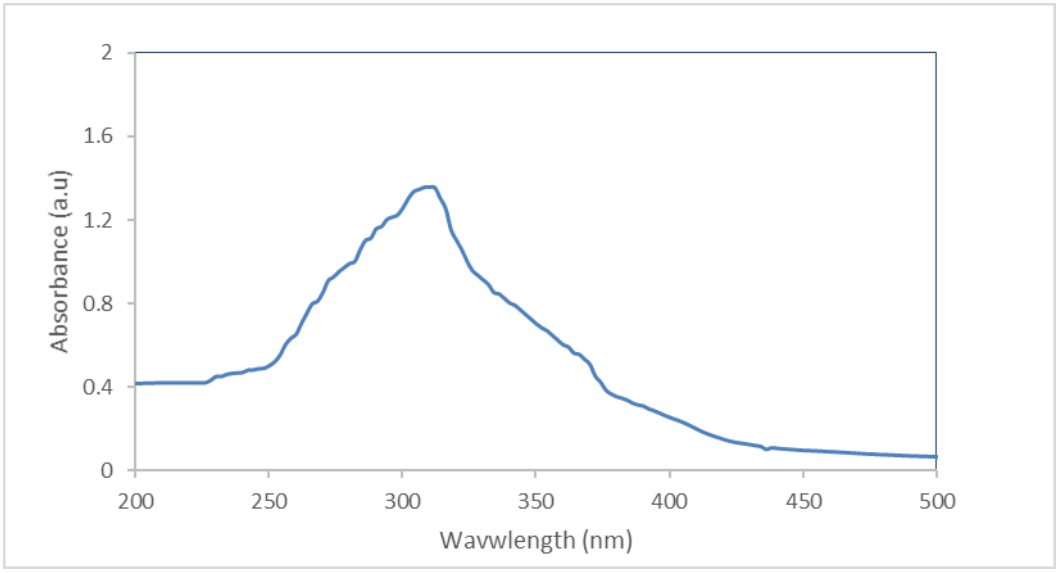

Figure (6): UV-Vis spectrum of Barium oxide nanoparticles

4-1-2-2 UV-visible of Nickel Oxide nanoparticles

The synthesized nickel nanoparticles' UV visible spectrum showed that the nickel oxide nanoparticles are accountable for the large absorption peak at 295 nm, and these results are similar to the results of researcher K.M. Racik et al [(10)]. The peak at 385 nm is most likely formed by Ni_2O_3, and this finding is similar to that of the researcher of M. Shaban et al [(11)].

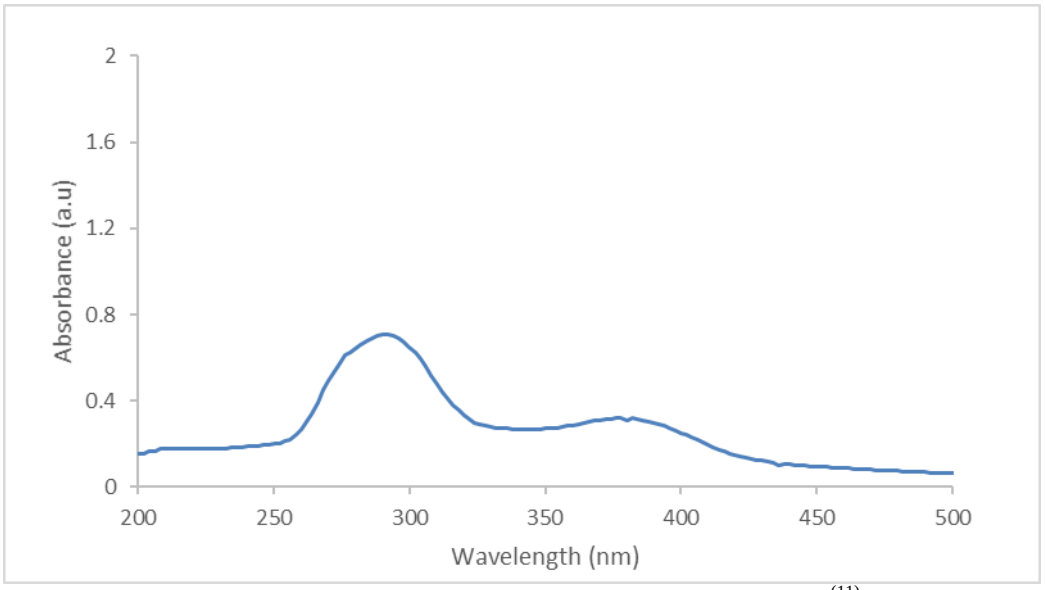

Figure (7): UV-Vis spectrum of Nickel oxide nanoparticles

4-1-3 X-ray diffraction analysis (XRD)

4-1-3-1 Barium Oxide Nanoparticle XRD Pattern

The XRD pattern of the BaO nanoparticles at the values of 22.69°, 24.68°, 25.65°, 28.52°, 31.22°, 40.4°, 48.15°, 56.25°, and 59.15° were ascribed to the (200), (201), (211), (102), (310), (111), (103), (211), (114). All of the reflection peaks can be easily indexed and well-matched with the tetragonal crystal structures phase of BaO nanoparticles and are in good agreement with the "JCPDS" card No. 26-0178 (134) [(9)]. The peaks occur at 2θ = 26.51°, 32.5°, 42.46°, and 68.5° with the hkl values (101), (212), (112), and (222) respectively, it resembles the presence of the body-centered structure of BaO_2 nanoparticles. The obtained values were well coincidental with the (JCPDS File No: 07-0233) (135) as shown in figure (8).

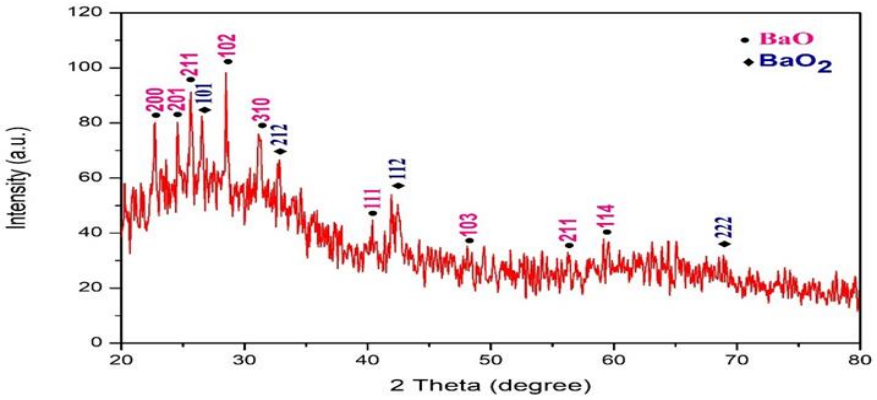

Figure (8): X-ray spectrum of Barium oxide nanoparticles.

The crystallite size diameter (D) of the BaO and BaO_2 nanoparticles has been calculated by Debye–Scherrer equation ($D = K\lambda/\beta\cos\theta$). The Crystallite size has been found to be 60.89 nm, as shown in table (1).

Table (1): The crystal size of the Barium oxides (BaO and BaO_2) nanoparticles.

Metal Oxide	2 Theta (degree)	FWHM (degree)	Cos theta	FWHM (rad)	D (nm)	Average
BaO	22.6941	0.15	0.980456291	0.002617801	54.10577	60.89
BaO	24.6871	0.3636	0.976886762	0.00634555	22.40242	
BaO	25.6506	0.2847	0.97505509	0.004968586	28.66464	
BaO_2	26.5182	0.2064	0.973346753	0.003602094	39.60826	
BaO	28.5261	0.2558	0.969179337	0.004464223	32.09655	
BaO	31.2245	0.4898	0.96311045	0.008547993	16.86818	
BaO_2	32.5146	0.0478	0.960020044	0.000834206	173.4023	
BaO	40.405	0.1667	0.938486924	0.00290925	50.86268	
BaO_2	42.4696	0.2142	0.932113874	0.00373822	39.85425	
BaO	48.15	0.09	0.913024883	0.001570681	96.83624	
BaO	56.25	0.09	0.881938307	0.001570681	100.2495	
BaO	59.1531	0.3083	0.869715783	0.005380454	29.67647	
BaO_2	68.5	0.09	0.826614528	0.001570681	106.959	

4-1-3-2 Nickel Oxide Nanoparticle XRD Pattern

The XRD pattern reflected the formation of Ni_2O_3 as the dominant phase of nickel oxide. The characteristic diffraction peaks of Ni_2O_3 were observed at 2θ angles of about 31.05° and 68.3° which are corresponding to (002) and (004) planes of hexagonal Ni_2O_3 (JCPDS Card Number 00-014-0481) [13]. The intense peaks in NiO nanoparticles at 2θ = 32.6, 34, and 64.5 degrees were associated with the (111), (100), and (220) crystalline planes [14]. The XRD pattern was in accordance with JCPDS card 04-0835, confirming that NiO nanoparticles are crystalline and have a pure face-centered cubic phase structure [15] as shown in figure (9). The average crystallite size (D) of Nickel Oxide nanoparticles was calculated based on Debye–Scherrer equation ($D = K\lambda/\beta\cos\theta$), where β FWHM (full-width at half-maximum or half-width) is in radian and θ is the position of the maximum of diffraction peak, K is the so-called shape factor, which usually takes a value of about 0.9, and λ is the X-ray wavelength (1.5406 Å for Cu Kα). The value of D is about 61.05 nm, as shown in table (2).

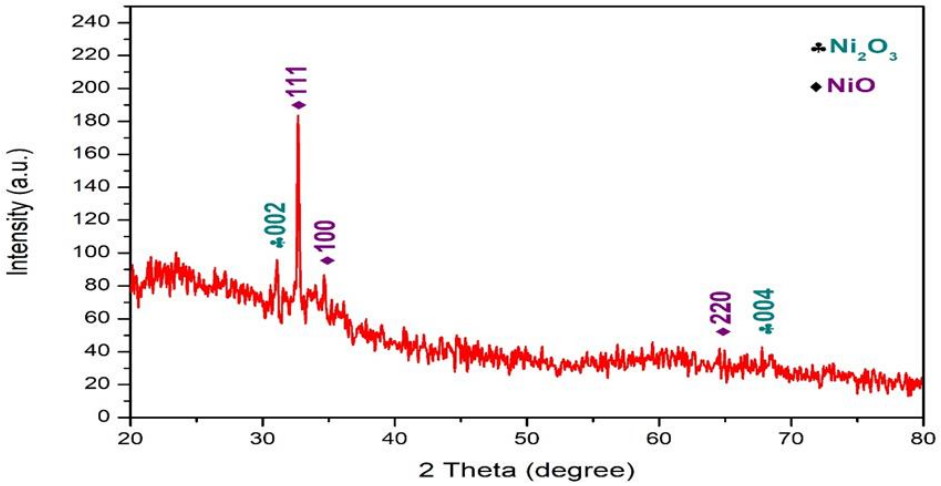

Figure (9): X-ray spectrum of nickel oxide nanoparticles.

Table (1): The crystal size of the nickel oxides (NiO and Ni_2O_3) nanoparticles.

Metal Oxide	2 Theta (degree)	FWHM (degree)	Cos theta	FWHM (rad)	D (nm)	Average
Ni_2O_3	31.0508	0.3812	0.96351723	0.006652705	21.6646	61.05
NiO	32.6884	0.2388	0.959594403	0.004167539	34.7249	
NiO	34.6	0.2223	0.954663047	0.003879581	37.49501	
NiO	64.55	0.09	0.845517063	0.001570681	104.5678	
Ni_2O_3	68.3	0.09	0.827595413	0.001570681	106.8323	

4-2 Characteristics of distilled products for Polypropylene by using Nanocomposites

We obtained the first liquid product for the distillation of polystyrene alone (PS) and also after adding the nickel oxide nanocomposite in different concentrations (25.3, 50.6, 75.9) ppm when distilling polystyrene at 280 °C. Also, after adding the barium oxide nanocomposite with different concentrations (25.9, 51.9, 77.8) ppm, as shown in Table (3).

Table (3): Characteristics of distilled products at 280°C Polystyrene.

parameter	PS	PS + 25.3 ppm of NiO	PS + 50.6 ppm of NiO	PS + 75.9 ppm of NiO	PS + 25.9 ppm of BaO	PS + 51.9 ppm of BaO	PS + 77.8 ppm of BaO
RON	104	104.7	104.6	104.4	104.8	104.6	104.5
MON	94	94.2	94.2	93.8	94.3	94.1	94
AKI	99	99.5	99.4	99.1	99.5	99.4	99.2
Density g\ml	0.892	0.887	0.883	0.868	0.885	0.882	0.872
Viscosity Pa.s	0.0135	0.0152	0.0121	0.0112	0.0121	0.0122	0.0173
volume	35	36	45	50	50	50	50
Flash point °C	44	47	51	50	48	48	45
Fire point °C	58	51	56	54	52	53	50
Aniline point °C	148	150	160	152	155	156	162
CET	0.0	0.0	0.0	0.0	0.0	0.0	0.0
Pour point °C	+0.0	+0.0	+0.0	+0.0	+0.0	+0.0	+0.0
Type	S	S	S	S	S	S	S
Time (hours)	2:30	2:00	2:10	2:00	2:15	1:45	1:00

The results of the decomposition of polystyrene at 280 °C by using two types of nanocomposites with different concentrations show us a liquid that has some high properties of the fuel because this type of polymer can be randomly broken to give chains with different lengths, branching, and molecular weight, and it can also break down sequentially to give the monomer component of it. The results of the decomposition of polystyrene at 280 °C by using two types of nanocomposites (NiO and BaO) show that the product increases in size with the increase of the nano-concentration, especially with 50 ml of BaO. The density and viscosity show a clear decrease with most concentrations, and on the contrary, the aniline point increases with increasing nano concentration until we reach 162 °C at a concentration of 77.8 ppm of BaO, and also the flash point increases with increasing nano concentration to reach 51 °C at a concentration of 50.6 ppm of NiO.

The results of the decomposition of polystyrene at 280 °C using two types of nanocomposites (NiO and BaO) showed that the value of the octane number increases, where its value at a concentration of 25.3 ppm of NiO is 104.7 and at a concentration of 25.9 ppm of BaO is 104.8, and this high increase is due to the aromatic content of the breakdown product originally present in the polymer structure. In contrast, the value of the cetane number was zero and also the fat content of the cracking product, and this indicates the sequential cracking of the polymer, and no long linear chains appeared. The results of the decomposition of polystyrene at 280 °C using two types of nanocomposites (NiO and BaO) showed that the decomposition time decreases with increasing nano-concentration of both nanocomposites, as it decreases from 2:30 hours for the original compound to 1:00 hours when using a concentration of 77.8 ppm of BaO.

We also obtained the second liquid product for the distillation of polystyrene alone (PS) and also after adding the nickel oxide nanocomposite in different concentrations (25.3, 50.6, 75.9) ppm when distilling polystyrene at 350 °C. Also, after adding the barium oxide nanocomposite with different concentrations (25.9, 51.9, 77.8) ppm, as shown in Table (4).

Table (4): Characteristics of distilled products at 350°C Polystyrene.

parameter	PS	PS + 25.3 ppm of NiO	PS + 50.6 ppm of NiO	PS + 75.9 ppm of NiO	PS + 25.9 ppm of BaO	PS + 51.9 ppm of BaO	PS + 77.8 ppm of BaO
RON	104.1	104.9	105	104.3	104.9	104.5	105
MON	94.2	94.4	94.6	93.9	94.4	94	94.5
AKI	99.1	99.6	99.8	99	99.6	99.3	99.7
Density g\ml	0.895	0.889	0.919	0.882	0.922	0.882	0.891
Viscosity Pa.s	0.0195	0.0132	0.0162	0.0101	0.0172	0.0162	0.0163
volume	50	50	32	31	35	35	35
Flash point °C	46	46	52	48	49	47	48
Fire point °C	52	50	56	52	52	52	54
Aniline point °C	145	155	162	160	162	162	163
CET	0.0	0.0	0.0	0.0	0.0	0.0	0.0
Pour point °C	+0.0	+0.0	+0.0	+0.0	+0.0	+0.0	+0.0
Type	S	S	S	S	S	S	S
Time (hours)	3:00	2:35	2:20	1:45	2:45	2:20	2:00

The results of the decomposition of polystyrene at 350 °C by using two types of nanocomposites with different concentrations show us a liquid that has some high properties of the fuel. The results of the decomposition of polystyrene at 350 °C by using two types of nanocomposites (NiO and BaO) show that the product decreases in size with increasing nano-concentration. As for the density and viscosity, they show a clear decrease with most concentrations except that they increase with concentrations of 50.6 ppm for NiO and 25.9 ppm for BaO, reaching 0.919 and 0.922, respectively. On the contrary, the aniline point increases with increasing nano concentration until we reach 163 °C at a concentration of 77.8 ppm of BaO, and also the flash point increases with increasing nano concentration to reach 52 °C at a concentration of 50.6 ppm of NiO. The results of the decomposition of polystyrene at 350 °C using two types of nanocomposites (NiO and BaO) showed that the value of the octane number increases, where its value reaching 105 at concentrations of 50.6 ppm for NiO and 77.8 ppm for BaO, as well as 104.9 for concentrations of 25.3 ppm for NiO and 25.9 ppm for BaO, this high increase is due to the aromatic content of the cracking product originally found in the polymer structure. In contrast, the value of the cetane number was zero and also the fat content of the cracking product. The results of the decomposition of polystyrene at 350 °C using two types of nanocomposites (NiO and BaO) showed that the decomposition time decreases with increasing nano-concentration of both nanocomposites, as it decreases from 3:00 hours for the original compound to 1:45 hours when using the concentration of 77.9 ppm of NiO and 2:00 hours when using the concentration of 77.8 ppm for BaO.

4- Conclusions

Through the results we reached in this study, we show the following important conclusions:

The ability to prepare nanoparticles through a homemade plasma system, with different concentrations (500, 1000, 1500, 2000 ppm)

eISSN 1303-5150

for nickel oxide and the best concentration we got was (2000 ppm), and the preparation of barium oxide with different concentrations (500, 1000, 1500, 2000, 2500, 2800 ppm) and the best concentration was (2800 ppm). When measured with X-rays, the size of barium nanoparticles (60.89 nm) and the size of nickel nanoparticles (61.05 nm). These nanoparticles can be used to prepare nanocomposites by mixing them with mineral salts. The possibility of using salt nanocomposites to improve the degradation of polymeric wastes into fuel with good properties.

The results of the decomposition of polystyrene at 280 °C using two types of nanocomposites (nickel oxide and Barium oxide) the Barium oxide nanocomposites showed better results than nickel oxide in terms of octane number, increase in size of fuel, and decomposition time. The cracking product cannot be similar to gasoline fuel because it has a high flash point and also does not have the value of the cetane number, so it cannot be close to diesel, but it can be used as an additive to raise the value of the octane number.

The results of the decomposition of polystyrene at 350 °C using two types of nanocomposites (nickel oxide and Barium oxide) the Barium oxide nanocomposites showed better results than nickel oxide in terms of octane number and aniline point, while the decomposition time is close for both compounds. In contrast, the value of the cetane number was zero and also the fat content of the cracking product, and this indicates the sequential cracking of the polymer, and no long linear chains appeared. Therefore, the cracking product cannot be similar to gasoline fuel because it has a high flash point and also does not have the value of the cetane number, so it cannot be close to diesel, but it can be used as an additive or domestic combustion fuel. The results showed that the time of deterioration of both polymers decreases with an increase in the concentration of the nanoparticles.

5- Acknowledgement

The authors gladly thank the technical and intellectual support for this work from the University of Anbar (www.uoanbar.edu.iq) and its esteemed academic staff.

References

1. Valavanidis, A., “Global Plastic Waste and Oceans’ Pollution. Million Tons of Plastic Waste Have Gone Missing in the World Oceans?”, Scientific Reports, Vol. 1, 1-39 (2016).

2. Alabi, O. A., Ologbonjaye, K. I., Awosolu, O., and Alalade, O. E., “Public and Environmental Health Effects of Plastic Wastes Disposal: A Review”, Journal of Toxicology and Risk Assessment, Vol. 5(1), (2019).

3. Tekman, M. B., Walther, B. A., Peter, C., Gutow, L. and Bergmann, M., “Impacts of plastic pollution in the oceans on marine species, biodiversity and ecosystems”, WWF Germany, Berlin, 1–221 (2022).

4. Wibawa, P. J., Agam, M. A., Nur, H., and Saim, H., “Changes in Physical Properties and Molecular Structure of Polystyrene Nanospheres Exposed with Solar Flux”, AIP Conference Proceedings, Vol. 1341, 54 (2011).

5. Natamai Subramanian, M., “Plastics Waste Management: Processing and Disposal”, Smithers Rapra Technology Ltd, 67-81 (2019).

6. Fridman, A., Chirokov, A. G., Gutsol, A., “Non-thermal atmospheric pressure discharges”, Journal of Physics D: Applied Physics, Vol. 38(2), R1–R24 (2005).

7. Sarker, M., Rashid, M. R., Rahman, M. S., and Molla M., “Polystyrene (PS) waste plastic conversion into aviation/kerosene category of fuel by using fractional column distillation process”, International Journal of Energy and Environment (IJEE), Vol. 3(6), 871-880 (2012).

8. Thawichsri, K., Nilnont, W., “A Simple Distillation Process Produce Fuel from Plastic Waste using Incorporate Heat Source”, International journal of advanced smart convergence, Vol. 4(1), 127-136 (2015).

9. Ansari, M. A., Jahan, N., “Structural and Optical Properties of BaO Nanoparticles Synthesized by Facile Co-Precipitation Method”, Materials Highlights, Vol. 2(1-2), 23–28 (2021).

10. Racik, K. M., Joseph, M., Raj, V. A., “Synthesis, Characterization and Optical Properties of Spherical NiO Nanoparticles”, National Laser Symposium (2018).

11. Shaban, M., Hamd, A., Amin, R. R., Abukhadra, M. R., Khalek, A. A., Khan, A. A. P., and Asiri, A. M., “Preparation and characterization of MCM-48/nickel oxide composite as an efficient and reusable catalyst for the assessment of photocatalytic activity”, Environmental Science and Pollution Research, Vol. 27(26), 32670-32682 (2020).

eISSN 1303-5150

12. Gomes, R., Roming, S., Przybilla, A., Meier, M. A. R., Feldmann, C., "Barium peroxide nanoparticles: Synthesis, characterization and their use for actuating the luminol chemiluminescence", Journal of Materials Chemistry C, Vol. 2(8), 1513-1518 (2014).

13. Aftab, M., Butt, M. Z., and Ali, D., "Effect of Molarity on the Structure, Optical Properties, and Surface Morphology Effect of Molarity on the Structure, Optical Properties, and Surface Morphology of (002) -Oriented Ni2O3 Thin Films Deposited via Spray Pyrolysis", Physical and Computational Sciences, Vol. 57(2), 51-74 (2020).

14. Yung, T. Y., Huang, L. Y., Chan, T. Y., Wang, K. S., Liu, T. Y., Chen, P. T., Chao, C. Y., and Liu, L. K., "Synthesis and characterizations of Ni-NiO nanoparticles on PDDA-modified graphene for oxygen reduction reaction", Nanoscale Research Letters, Vol. 9(1), 1-6 (2014).

15. Iqbal, A., Haq, A. U., Cerrón-Calle, G. A., Naqvi, S. A. R., Westerhoff, P. and Garcia-Segura, S., "Green synthesis of flower-shaped copper oxide and nickel oxide nanoparticles via Capparis decidua leaf extract for synergic adsorption-photocatalytic degradation of pesticides", Catalysts, Vol. 11(7), 806 (2021).